Published in final edited form as:
Biochemistry. 2008 April 22; 47(16): 4575–4582. doi:10.1021/bi8001743.

A Substrate in Pieces: Allosteric Activation of Glycerol 3-Phosphate Dehydrogenase (NAD+) by Phosphite Dianion†

Wing-Yin Tsang, **Tina L. Amyes**, and **John P. Richard**‡
Department of Chemistry, University at Buffalo, SUNY, Buffalo, New York, 14260-3000

Abstract

The ratio of the second-order rate constants for reduction of dihydroxyacetone phosphate (DHAP) and of the neutral truncated substrate glycolaldehyde (GLY) by glycerol 3-phosphate dehydrogenase (NAD^+, GPDH) saturated by NADH is $(1.0\times10^6\ M^{-1}\ s^{-1})/(8.7\times10^{-3}\ M^{-1}\ s^{-1}) = 1.1\times10^8$, which was used to calculate an intrinsic phosphate binding energy of ≤ −11.0 kcal/mol. Phosphite dianion binds very weakly to GPDH (K_d > 0.1 M), but the bound dianion strongly activates GLY towards enzyme-catalyzed reduction by NADH. Thus, the large intrinsic phosphite binding energy is expressed *only* at the transition state for the GPDH-catalyzed reaction. The ratio of rate constants for the phosphite-activated and the unactivated GPDH-catalyzed reduction of GLY by NADH is $(4300\ M^{-2}\ s^{-1})/(8.7\times10^{-3}\ M^{-1}\ s^{-1}) = 5\times10^5\ M^{-1}$, which was used to calculate an intrinsic phosphite binding energy of −7.7 kcal/mol for the association of phosphite dianion with the transition state complex for the GPDH-catalyzed reduction of GLY. Phosphite dianion has now been shown to activate bound substrates for enzyme-catalyzed proton transfer, decarboxylation, hydride transfer and phosphoryl transfer reactions. Structural data provides strong evidence that enzymic activation by the binding of phosphite dianion occurs at a modular active site featuring: (1) a binding pocket complementary to the reactive substrate fragment, and which contains all the active site residues needed to catalyze the reaction of the substrate piece or of the whole substrate; (2) a phosphate/phosphite dianion binding pocket that is completed by the movement of flexible protein loop(s) to surround the nonreacting oxydianion. We propose that loop motion and associated protein conformational changes that accompany the binding of phosphite dianion and/or phosphodianion substrates leads to encapsulation of the substrate and/or its pieces in the protein interior, and to placement of the active site residues in positions where they provide optimal stabilization of the transition state for the catalyzed reaction.

Enzymes are protein catalysts that effect much larger rate accelerations than those observed for small molecule catalysts. The larger rate accelerations for enzymes are a consequence of the greater binding affinities of enzymes for their reaction transition states (1). Enzyme catalysis is so efficient that the release of products would be intolerably slow if they were to bind with the same affinity as the transition state. For example, the ca. 30 kcal/mol transition state intrinsic binding energy estimated for the enzymatic decarboxylation of orotidine 5′-monophosphate (OMP)[1] catalyzed by orotidine 5′-monophosphate decarboxylase (OMPDC) (2) is even larger than the 20 kcal/mol binding energy associated with the effectively irreversible binding of biotin to avidin (3). Consequently, in order to avoid this free energy "trap", enzymes generally bind their substrates/products much more weakly than the reaction transition state.

†This work was supported by Grant GM39754 from the National Institutes of Health.

‡To whom correspondence should be addressed, *Tel:* (716) 645 6800 ext 2194, *Fax:* (716) 645 6963, *Email:* jrichard@chem.buffalo.edu.

[1]Abbreviations: OMP, orotidine 5'-monophosphate; OMPDC, orotidine 5'-monophosphate decarboxylase; GAP, (*R*)-glyceraldehyde 3-phosphate; TIM, triosephosphate isomerase; GPDH, glycerol 3-phosphate dehydrogenase (NAD^+); DHAP, dihydroxyacetone phosphate; NADH, nicotinamide adenine dinucleotide, reduced form; α-GP, L-glycerol 3-phosphate; GLY, glycolaldehyde; BSA, bovine serum albumin; DTT, D,L-dithiothreitol; TEA, triethanolamine; NMR, nuclear magnetic resonance.

It has been proposed that enzymes often achieve large rate accelerations through the utilization of binding interactions between the protein and nonreacting portions of the substrate for transition state stabilization (4,5). However, the mechanism(s) by which enzyme catalysts selectively "turn on" these binding interactions at the transition state for their catalyzed reactions is not generally known, and this question is often omitted from discussions of the origin of the rate acceleration for enzyme catalysts.

The binding energy of the remote nonreacting phosphodianion groups of OMP and (*R*)-glyceraldehyde 3-phosphate (GAP) has been shown to provide a ca. 12 kcal/mol stabilization of the transition states for OMPDC-catalyzed decarboxylation (6) and proton transfer catalyzed by triosephosphate isomerase (TIM) (7), respectively. Moreover, the small substrate "piece" phosphite dianion provides strong allosteric-like activation of OMPDC-catalyzed decarboxylation (6) and TIM-catalyzed deprotonation (8) of a second truncated substrate piece from which the phosphodianion group has been excised. The latter results show that a substantial fraction of the "intrinsic phosphate binding energy" is expressed as transition state stabilization even in the *absence* of a covalent connection between the substrate pieces. Phosphite dianion binds weakly to both TIM (K_d = 38 mM) (8) and OMPDC (K_d = 140 mM) (6), so that the large intrinsic phosphite binding energy is expressed only at the respective transition states for these enzyme-catalyzed reactions.

X-ray crystallographic analyses suggest that both TIM and OMPDC *utilize* the binding energy of the substrate phosphodianion group to drive the thermodynamically unfavorable closure of a mobile protein loop(s) to cover the bound phosphodianion (9–12). We have proposed (8) that this loop closure sequesters the substrate from bulk solvent and results in formation of a local microenvironment in which there is optimal stabilization of transition state for the enzymatic reaction (13,14).

We examine here whether the functional equivalence of GAP and the "two-part substrate" [glycolaldehyde + phosphite] (Scheme 1) for proton transfer catalyzed by TIM might also be observed for other types of enzymatic reactions. Glycerol 3-phosphate dehydrogenase (NAD^+-linked, EC. 1.1.1.8., GPDH) is used in the assay for TIM-catalyzed isomerization of GAP to couple formation of the product dihydroxyacetone phosphate (DHAP) to its reduction by NADH to give L-glycerol 3-phosphate (α-GP, Scheme 2) (15). We report here that GPDH also catalyzes the very slow reduction of the neutral minimal substrate glycolaldehyde (GLY) by NADH, and that the *separate* binding of the second substrate piece phosphite dianion strongly activates GPDH for catalysis of the reduction of GLY by NADH. We conclude that the substrate pieces [glycolaldehyde + phosphite] are able to effectively substitute for the whole substrate GAP or DHAP in enzyme-catalyzed proton transfer and hydride transfer reactions, respectively.

MATERIALS AND METHODS

Materials

Glycerol 3-phosphate dehydrogenase (lyophilized powder, 75 units/mg) from rabbit muscle was purchased from USB Corporation. Bovine serum albumin, Fraction V (BSA) was from Roche. Dihydroxyacetone phosphate (lithium salt), NADH (disodium salt), glycolaldehyde dimer, triethanolamine hydrochloride, D,L-dithiothreitol (DTT) and sodium deuteroxide (40 wt %, 99.9% D) were from Sigma-Aldrich. Deuterium oxide (99.9% D) was from Cambridge Isotope Laboratories. Sodium phosphate (dibasic) was from Fluka and sodium phosphite (dibasic, pentahydrate) was from Riedel-de Haen (Fluka). Water was from a Milli-Q Academic purification system. All other chemicals were reagent grade or better and were used without further purification.

Preparation of Solutions

Solution pH was determined as described previously (8). Stock solutions of NADH were prepared by dissolving NADH (disodium salt) in water and were stored at 4 °C. The concentration of NADH was determined spectrophotometrically at 340 nm using ε = 6220 M^{-1} cm^{-1}. Stock solutions of DHAP were prepared on the day of the experiment by dissolving the lithium salt in water and adjusting to pH 7.5 using 1 M NaOH and were stored on ice. The concentration of DHAP was determined spectrophotometrically at 340 nm as the concentration of NADH oxidized in a reaction catalyzed by GPDH. GPDH (2 or 20 mg/mL) in 20 mM triethanolamine (TEA) buffer (pH 7.5, 32% free base) was dialyzed exhaustively against the same buffer at 5 °C. The concentration of GPDH was determined from the absorbance at 280 nm using A = 5.15 for a 1% solution of GPDH (16) and a subunit molecular weight of 37,500 Daltons. Stock solutions of glycolaldehyde (100 mM monomer) were prepared by dissolving glycolaldehyde dimer in water and storing the solution for at least three days at room temperature to allow for break down of the dimer to give the monomer (8). An apparent pK_a of 6.38 for phosphite monoanion at 25 °C and I = 0.12 (NaCl) was determined as the pH of a 30 mM solution of the sodium salt at a 1:1 monoanion:dianion ratio.

Enzyme Assays

Dilutions of the dialyzed stock solutions of 2 mg/mL enzyme (used for assays of GPDH-catalyzed reduction of DHAP) and 20 mg/mL enzyme (used for assays of GPDH-catalyzed reduction of GLY) were made into 20 mM TEA (pH 7.5, 32% free base) containing 10 mM DTT.

All enzyme assays were conducted at 25 °C and I = 0.12 (NaCl) in a volume of 1 mL. Initial velocities of oxidation of NADH (≤ 5% reaction) were calculated from the changes in absorbance at 340 nm using Δε = 6220 M^{-1} cm^{-1}. The standard assay mixture for GPDH activity contained 100 mM TEA (pH 7.5), 1.2 mM DHAP, 0.20 mM NADH, 0.1 mg/mL BSA, 50 μM DTT and ca. 1 nM GPDH at I = 0.12 (NaCl). Reactions were initiated by making a 200-fold dilution of the diluted stock enzyme containing 10 mM DTT into the reaction mixture. The same procedure was used to determine the velocity of GPDH-catalyzed reduction over a range of initial concentrations of DHAP, except that the buffer was 20 mM TEA (pH 7.5).

Assay mixtures for the GPDH-catalyzed reduction of GLY in the *absence* of phosphate contained 10 mM TEA (pH 7.5), 20 mM GLY (total), 0.20 mM NADH and up to ca. 0.2 mM GPDH at I = 0.12 (NaCl). Assay mixtures for the GPDH-catalyzed reduction of GLY in the *presence* of phosphite contained 10 mM TEA (pH 7.5), 2 – 60 mM GLY (total), 0.20 mM NADH, up to 32 mM phosphite dianion and 0.6 μM GPDH at I = 0.12 (NaCl).

^{1}H NMR Analyses

^{1}H NMR spectra at 500 MHz were recorded in D_2O at 25 °C using a Varian Unity Inova 500 spectrometer as described previously (8). The product of the GPDH-catalyzed reduction of GLY by NADH in a reaction mixture containing 10 mM TEA at pD 8.0, 31 mM sodium phosphite (93% dianion), 5 mM GLY (total) and 7 mM NADH in D_2O was identified by ^{1}H NMR spectroscopy. The reaction was initiated by the addition of 380 μL of GPDH in buffered D_2O (pD 8.0, 20 mM TEA) to give a total volume of 1 mL and a final enzyme concentration of 11 μM. A second ^{1}H NMR spectrum, obtained after a reaction time of 12 hours, showed the disappearance of ca. 80% of the starting GLY and the appearance of a singlet at 3.53 ppm, which was shown to be due to the methylene protons of a corresponding amount of ethylene glycol by the addition of an authentic standard.

The fraction of GLY present in the *free carbonyl* form in H_2O buffered by 10 mM TEA (pH 7.5) at 25 °C and I = 0.12 (NaCl), (1 - f_{hyd}), was determined by ^{1}H NMR spectroscopy using

a coaxial inner tube containing D_2O and suppression of the water peak. A value of $(1 - f_{hyd}) = 0.06 \pm 0.003$ was obtained by comparison of the integrated areas of the signals due to the C2-protons of the free carbonyl and hydrated forms of GLY, which is the same as $(1 - f_{hyd}) = 0.06$ determined previously for the hydration of GLY in D_2O at pD 7.0, 25 °C and $I = 0.10$ (8).

RESULTS

Initial velocities, v_i, of the reduction of DHAP by NADH catalyzed by GPDH at pH 7.5 (10 mM TEA), 25 °C and $I = 0.12$ (NaCl) were determined by monitoring the decrease in absorbance at 340 nm. Figure 1A shows the dependence of v_i ($M\ s^{-1}$) on the total concentration of DHAP in the presence of 0.10 mM (▲) or 0.20 mM (●) NADH and 1.1 nM GPDH. The solid line shows the fit of the data to the Michaelis-Menten equation with values of $(K_m)_{app} = 0.24$ mM and $V_{max} = 1.42\times10^{-7}$ M s^{-1}. The latter was used to calculate $k_{cat} = 130\ s^{-1}$, and a value of $K_m = 0.13$ mM for the reactive *free carbonyl* form of DHAP was calculated using $(1 - f_{hyd}) = 0.55$ for the fraction of DHAP present in the free carbonyl form (Scheme 3) (17). These data (Table 1) are in agreement with the published kinetic parameters for GPDH (18).

There is a ca. 50% decrease in the activity of GPDH (60 μM) during an eight hour incubation at pH 7.5 (10 mM TEA) in the presence of 1.2 mM GLY (free carbonyl form, 20 mM total GLY) and 0.20 mM NADH at 25 °C and $I = 0.12$ (NaCl). Figure 1B shows the dependence of the initial velocity v_i ($M\ s^{-1}$) of the reduction of GLY under these conditions on the concentration of GPDH, determined from the decrease in absorbance at 340 nm (0.01 − 0.02 OD units) observed at early reaction times (≤ 60 minutes) where the velocity is constant. The loss of activity of GPDH during this time, determined by periodic standard assay, was less than 10%. The slope of the correlation in Figure 1B gives the apparent first-order rate constant for the enzymatic reduction of GLY as $(1.04 \pm 0.06)\times10^{-5}\ s^{-1}$.[2] The second-order rate for enzyme-catalyzed reduction of GLY (Scheme 3) can then be calculated as $(k_{cat}/K_m)_{GLY} = (1.04\times10^{-5}\ s^{-1})/[GLY] = (8.7 \pm 0.5)\times10^{-3}\ M^{-1}\ s^{-1}$, where [GLY] = 1.2 mM is the concentration of GLY present in the reactive free carbonyl form.

Figure 2A shows that there is a *linear* dependence of $v_i/[E]$ (s^{-1}) for the reduction of various concentrations of GLY by NADH (0.20 mM) catalyzed by GPDH (0.6 μM) on the concentration of exogenous phosphite dianion at pH 7.5 (10 mM TEA), 25 °C and $I = 0.12$ (NaCl). The addition of phosphite dianion results in very large increases in v_i for these GPDH-catalyzed reactions and ^1H NMR analysis confirmed that the product of the reduction of GLY by NADH in the presence of phosphite dianion is ethylene glycol (Scheme 4). The failure to observe curvature in the correlations shown in Figure 2A requires that phosphite dianion bind very weakly to GPDH so that the concentrations of both the ternary complex E•NADH•HPO_3^{2-} and the quaternary complex E•NADH•GLY•HPO_3^{2-} are each much smaller than the total concentration of GPDH over the range of [HPO_3^{2-}] examined. The data were therefore fit to eq 1, derived for a reaction mechanism in which there is no significant formation of the E•NADH•HPO_3^{2-} complex (Scheme 4). The linear correlations in Figure 2A show that [HPO_3^{2-}] « K_b and the slopes of these correlations correspond to apparent second-order rate constants $(k_{cat}/K_m)_{app}$ ($M^{-1}\ s^{-1}$) for the phosphite-activated GPDH-catalyzed reduction of GLY by NADH (eq 2).

$$v_i/[E] = \frac{k_{cat}[GLY][HPO_3^{2-}]}{[GLY][HPO_3^{2-}] + K_b[GLY] + K_{ia}K_b} \quad (1)$$

[2]Quoted errors are standard deviations obtained from the linear or nonlinear least squares fit of the data. Errors in calculated quantities were computed using standard equations for the propagation of error.

$$(k_{cat}/K_m)_{app} = \frac{(k_{cat}/K_b)[GLY]}{K_{ia} + [GLY]} \quad (2)$$

Figure 2B shows the dependence of $(k_{cat}/K_m)_{app}$, determined as the slopes of the correlations in Figure 2A, on the concentration of the *free carbonyl* form of glycolaldehyde. The solid line shows the fit of the data to eq 2, which gave values of $K_{ia} = 8 \pm 1$ mM for binding of GLY and $k_{cat}/K_b = 35 \pm 4$ M^{-1} s^{-1} (Scheme 4). The slope of the correlation in Figure 2B at *low concentrations* of GLY corresponds to the *third-order* rate constant $k_{cat}/K_{ia}K_b = 4300 \pm 700$ M^{-2} s^{-1} for the phosphite-activated GPDH-catalyzed reduction of GLY by NADH. The kinetic parameters determined in this work are summarized in Table 1.

The velocity of the GPDH-catalyzed reduction of DHAP by NADH (0.20 mM) at [DHAP] = K_m, pH 7.5 (10 mM TEA), 25 °C and $I = 0.12$ (NaCl) was found to decrease by 15% upon the inclusion of 33 mM phosphite dianion, while 35 mM sulfate dianion causes a somewhat larger 36% decrease in the velocity under the same reaction conditions. These small changes in velocity show that both phosphite and sulfate dianions bind only weakly to GPDH. The evaluation of binding constants K_i for these dianions is complicated by uncertainties in whether there are also specific salt effects on the kinetic parameters for the GPDH-catalyzed reaction.

DISCUSSION

The cofactor NAD^+ is a competitive product inhibitor of the GPDH-catalyzed reduction of DHAP when NADH is the varied substrate but a noncompetitive inhibitor when DHAP is the varied substrate (19). The sugar L-glycerol 3-phosphate is a noncompetitive product inhibitor of the GPDH-catalyzed reduction of DHAP when either NADH or DHAP is the varied substrate; but, the inhibition with respect to NADH changes to uncompetitive when the reaction is carried out in the presence of saturating concentrations of DHAP (19). These results provide strong evidence for an ordered mechanism, with NADH binding first followed by DHAP (18,19). A similar ordered mechanism is assumed to hold for reduction of the "two-part substrate" [glycolaldehyde + phosphite] by NADH, with the cofactor binding first, followed by binding of the substrate pieces GLY and phosphite dianion (Scheme 4). A Michaelis constant of 6.3 μM for NADH has been reported for the GPDH-catalyzed reduction of DHAP at pH 7.8 (19). The essentially identical dependence of the initial velocity of GPDH-catalyzed reduction on [DHAP] in the presence of 0.10 mM or 0.20 mM NADH at pH 7.5 (Figure 1A) shows that under our reaction conditions GPDH is completely saturated by the lower concentration of NADH. Studies of the reduction of GLY and of the phosphite-activated reduction of GLY catalyzed by GPDH were carried out in the presence of 0.20 mM NADH so that the concentration of the E•NADH complex is given by the total concentration of enzyme.

Reaction of the Substrate in Pieces

The Michaelis-Menten plots for the reduction of DHAP catalyzed by GPDH at [NADH] = 0.10 or 0.20 mM and pH 7.5 (Figure 1A) give $K_m = 0.13$ mM for the *free carbonyl* form of DHAP and $k_{cat}/K_m = 1.0 \times 10^6$ M^{-1} s^{-1} as the second-order rate constant for reduction of DHAP by the E•NADH complex. By comparison, a value of $(k_{cat}/K_m)_{GLY} = (8.7 \pm 0.5) \times 10^{-3}$ M^{-1} s^{-1} was determined for reduction of the truncated substrate GLY by the E•NADH complex (Figure 1B). We conclude that the substrate phosphodianion group activates DHAP towards GPDH-catalyzed reduction by NADH by at least 10^8-fold. This likely underestimates the phosphodianion group activation because the aldehyde group of GLY is intrinsically more reactive towards a nucleophilic hydride donor than is the keto group of DHAP. These data show that the enzymatic transition state for hydride transfer from enzyme-bound NADH to

DHAP is stabilized by at least 11 kcal/mol by interactions between GPDH and the nonreacting phosphodianion group of the substrate (Table 2).

The GPDH-catalyzed reduction of GLY by NADH is strongly activated by the second substrate piece phosphite dianion. Figure 2A shows that plots of $v_i/[E]$ (s^{-1}) for reduction of various concentrations of GLY by NADH (0.20 mM) at pH 7.5 (I = 0.12, NaCl) against [HPO_3^{2-}] are linear up to at least 33 mM phosphite dianion. The same concentration of phosphite dianion results in only a 15% reduction in the initial velocity of GPDH-catalyzed reduction of DHAP by NADH at [DHAP] = K_m. We conclude that phosphite dianion binds only weakly to GPDH (K_d > 0.1 M for dissociation of the E•HPO_3^{2-} complex), but that this dianion provides an impressive activation of reduction of the second substrate piece GLY by NADH catalyzed by GPDH.

The slopes of the linear correlations in Figure 2A correspond to apparent second-order rate constants $(k_{cat}/K_m)_{app}$ for the phosphite-activated reduction of GLY catalyzed by the E•NADH complex. Figure 2B shows that these apparent second-order rate constants appear to approach a limiting value for reactions at high concentrations of the hydride acceptor GLY. The fit of the data in Figure 2B to eq 2 (derived for Scheme 4) gave $k_{cat}/K_{ia}K_b$ = 4300 ± 700 M^{-2} s^{-1} as the third-order rate constant for reaction of the two substrate pieces GLY and HPO_3^{2-} with E•NADH to form ethylene glycol and NAD^+. Scheme 5 shows that the intrinsic affinity of HPO_3^{2-} for the GPDH-transition state complex E•S‡, defined as K_d‡ = 2 μM for the E•HPO_3^{2-}•S‡ complex, can be calculated as the ratio of the second-order rate constant for unactivated enzyme-catalyzed reduction of GLY, $(k_{cat}/K_m)_{GLY}$, and the *third-order* rate constant for reaction of the substrate pieces, $k_{cat}/K_{ia}K_b$, according to eq 3.

$$K_d^{\ddagger}=\frac{(k_{cat}/K_m)_{GLY}}{k_{cat}/K_{ia}K_b}=\frac{0.0087\ M^{-1}s^{-1}}{4300\ M^{-2}s^{-1}}=2.0\ \mu M \quad (3)$$

The observation of linear plots in Figure 2A for the phosphite-activated enzyme-catalyzed reduction of GLY by NADH shows that there is no detectable accumulation of the E•HPO_3^{2-} complex at [HPO_3^{2-}] ≤ 33 mM. Therefore, the binding of phosphite dianion to the free enzyme is not shown in Scheme 5, because the stability of E•HPO_3^- relative to the free enzyme is not defined by our experiments.

Scheme 5 is represented graphically in Figure 3A. The large activation barrier of ca. 20 kcal/mol for the direct bimolecular reduction of the truncated neutral substrate GLY by the E•NADH complex was calculated from the second-order rate constant $(k_{cat}/K_m)_{GLY}$ = (8.7 ± 0.5) ×10^{-3} M^{-1} s^{-1} (Table 1) using the Eyring equation at 298 K. The smaller activation barrier for the phosphite-activated reduction of GLY was calculated from the third-order rate constant $k_{cat}/K_{ia}K_b$ = 4300 ± 700 $M^{-2}s^{-1}$ (Table 1). The 7.7 kcal/mol larger activation barrier for reduction of GLY catalyzed by E•NADH compared to its phosphite-activated reduction is equal to the stabilization associated with the binding of phosphite dianion to the transition state complex E•S‡ to give E•HPO_3^{2-}•S‡ for which $K_d^{\ddagger}$ = 2 μM.

Mobile Loops and Catalysis

X-ray crystallographic analysis of GPDH from *Leishmania mexicana* shows that the GPDH•NAD^+•DHAP ternary complex adopts a "closed" form relative to the free, unliganded, enzyme (20). It has been proposed that the formation of stabilizing interactions between the phosphodianion group of bound DHAP and amino acid side-chains at mobile protein elements provides the major driving force for closure of the protein pocket (20,21). This is analogous to the closure of flexible loops around the phosphodianion group of bound intermediate analogs at TIM (11,12,22) and at OMPDC (9,23). In these cases, loop closure and the formation of

interactions with the substrate phosphodianion group were proposed to activate the substrates GAP/DHAP and OMP for the respective enzyme-catalyzed proton transfer (8) and decarboxylation (6) reactions.

Figure 3B is a free energy diagram that illustrates one physical mechanism for activation of GPDH towards reduction of glycolaldehyde by the binding of exogenous phosphite dianion. In this model we propose that a large fraction of the intrinsic binding energy of −7.7 kcal/mol for the phosphite dianion activator is *utilized* to drive a thermodynamically unfavorable change in the conformation of the enzyme from an inactive open form E'_O (E' = E•NADH) to an active loop-closed form E'_C. The *observed* binding of phosphite dianion to the free enzyme is therefore only weakly favorable, with a binding energy×> −1.4 kcal/mol, because the total intrinsic phosphite binding energy is largely offset by the unfavorable free energy associated with the conformational changes that accompany binding of this substrate piece, $\Delta G_{conf} = 7.7 + \times$ kcal/mol. We also propose that a large fraction of the intrinsic binding energy of the transition state for reduction of the neutral substrate piece GLY, $S^{\ddagger}$, is utilized to drive the same loop closure and conformational change. The *full* intrinsic binding energy of HPO_3^{2-} or of the transition state $S^{\ddagger}$ is then observed *only* when these species bind to the loop-closed forms of GPDH, E'_C•$S^{\ddagger}$ or E'_C•HPO_3^{2-}, respectively.

We propose that the large selectivity of phosphite dianion for binding to E'_C rather than to E'_O results from the formation of stabilizing interactions between this oxydianion and amino acid side-chains at mobile protein elements that move to form the loop-closed protein, and that very similar interactions are formed between the protein and the phosphodianion group of the whole substrate DHAP. The proposed large selectivity of the transition state for binding to E'_C would require that loop closure results in formation of a local environment that is *more favorable* for transformation of the bound substrate to the transition state for hydride transfer than that at the open enzyme E'_O. We are able only to speculate about these changes, because the imperatives for enzymatic catalysis of hydride transfer from NADH have not been well defined.

Loop closure that sequesters the substrate from aqueous solvent at a nonpolar active site should have the effect of increasing the extent of transition state stabilization available from hydrogen-bonding and ion-pairing interactions between the protein and the bound ligand (24). For example, the magnitude of the stabilizing electrostatic interactions between enzymic hydrogen bond donors and the partial negative charge that develops at the carbonyl oxygen in the transition state for hydride transfer from NADH to glycolaldehyde will increase with a decrease in the effective dielectric constant of the reaction medium (25). It is possible that loop closure upon substrate binding to GPDH results in a decrease in the separation between the hydride donor and the hydride acceptor at the Michaelis complex. This would narrow the width of the potential energy barrier that separates reactants and products, and it could favor quantum mechanical tunneling through this barrier (26). Finally, loop closure may have the effect of "ordering" the catalytic groups in the active site to provide optimal transition state stabilization by minimizing the entropic barrier to the enzyme-catalyzed reaction (13).

How do Enzymes Work?

Glucose 1-phosphate and glucose 6-phosphate are rapidly phosphorylated by the phosphoserine of phosphoglucomutase to form glucose 1,6-diphosphate. In 1976 Bill Ray showed that enzyme-catalyzed phosphorylation of xylose by this enzyme is very slow, but that this phosphoryl transfer reaction is strongly activated by binding of the second substrate piece phosphite dianion (27). It has taken 30 years to generalize these results from studies of an enzyme-catalyzed phosphoryl group transfer reaction to enzyme-catalyzed proton transfer (8), hydride transfer (this work) and decarboxylation reactions (6). Our work on three different enzymes that catalyze mechanistically diverse heterolytic reactions has shown that these

catalysts have achieved strikingly similar efficiencies in their utilization of the intrinsic binding energy of the substrate phosphodianion group in catalysis (Table 2).

(1) OMPDC, TIM and GPDH show similar $10^8 - 10^9$-fold lower activities for catalysis of the reaction of a truncated substrate that lacks a phosphodianion group, $(k_{cat}/K_m)_S$, than for catalysis of the reaction of the whole substrate, $(k_{cat}/K_m)_{SPi}$ These results suggest that an important outcome of the biological phosphorylation of sugars is to provide enzyme catalysts with an electrostatic *handle* from which they may obtain ca. 12 kcal/mol of intrinsic binding energy.

(2) Each of these very slow enzyme-catalyzed reactions of the appropriate truncated neutral substrate piece is strongly activated by the separate binding of exogenous phosphate dianion.

(3) In each case the second-order rate constant $(k_{cat}/K_m)_{SPi}$ for reaction of the "whole" substrate is larger than the third-order rate constant for the phosphite-activated reaction of the truncated substrate piece ($4300 - 12{,}000\ M^{-2}\ s^{-1}$, see Table 2). The difference between the second-order rate constant for reaction of the whole substrate and the third-order rate constant for reaction of the pieces reflects the large entropic advantage to the unimolecular reaction of the whole substrate, compared with the bimolecular reaction of the pieces (28).

(4) The individual substrate pieces exhibit low affinities for the formation of productive Michaelis complexes. However, tethering the two pieces gives a whole substrate that exhibits an enhanced binding affinity due to the chelate effect (28).

(5) In each case binding of the substrate phosphodianion group drives the movement of mobile protein loop(s) to close the active site and cover the phosphate group, which effectively buries the reactive substrate fragment in the protein interior. The binding of phosphite dianion presumably drives a similar conformational change (8).

Apparently, these diverse proteins have adopted a common modular design in order to effect very efficient enzymatic catalysis from utilization of the intrinsic binding energy of the nonreacting phosphate fragment of the substrate. This design features: (a) An active site that recognizes the reactive substrate fragment and which contains all of the catalytic amino acid side-chains needed to execute the chemistry of catalyzed reaction. (b) A neighboring site for a second *nonreactive* substrate piece (for example, phosphite dianion), which is completed by the movement of flexible protein loops over this piece. This loop movement encapsulates the *reactive* substrate piece within the protein where the local dielectric constant is smaller than that of water, the catalytic side chains are positioned to provide optimal transition state stabilization, and where other electrostatic factors may also favor transition state stabilization.

In recent years there have been, at best, small incremental advances in the *de novo* rational design of synthetic small molecule catalysts or of large molecular weight protein or nucleic acid catalysts. We suggest that the recognition and understanding of this modular design element in enzymes that have evolved to effectively utilize "intrinsic phosphate binding energy" may guide the efforts of chemical biologists interested in the *de novo* design of proteins with enzyme-like catalytic activities.

REFERENCES

1. Pauling L. The nature of forces between large molecules of biological interest. Nature 1948;161:707–709. [PubMed: 18860270]
2. Radzicka A, Wolfenden R. A proficient enzyme. Science 1995;267:90–93. [PubMed: 7809611]
3. Green NM. Thermodynamics of the binding of biotin and some analogues by avidin. Biochem. J 1966;101:774–780. [PubMed: 16742458]

4. Jencks WP. Binding Energy, Specificity and Enzymic Catalysis: The Circe Effect. Adv. Enzymol. Relat. Areas Mol. Biol 1975;43:219–410. [PubMed: 892]
5. Jencks WP. Economics of enzyme catalysis. Cold Sp. Har. Sym. Quant. Biol 1987;52:65–73.
6. Amyes TL, Richard JP, Tait JJ. Activation of orotidine 5'- monophosphate decarboxylase by phosphite dianion: The whole substrate is the sum of two parts. J. Am. Chem. Soc 2005;127:15708–15709. [PubMed: 16277505]
7. Amyes TL, O'Donoghue AC, Richard JP. Contribution of phosphate intrinsic binding energy to the enzymatic rate acceleration for triosephosphate isomerase. J. Am. Chem. Soc 2001;123:11325–11326. [PubMed: 11697989]
8. Amyes TL, Richard JP. Enzymatic catalysis of proton transfer at carbon: activation of triosephosphate isomerase by phosphite dianion. Biochemistry 2007;46:5841–5854. [PubMed: 17444661]
9. Miller BG, Hassell AM, Wolfenden R, Milburn MV, Short SA. Anatomy of a proficient enzyme: the structure of orotidine 5'-monophosphate decarboxylase in the presence and absence of a potential transition state analog. Proc. Natl. Acad. Sci. U. S. A 2000;97:2011–2016. [PubMed: 10681417]
10. Miller BG, Snider MJ, Short SA, Wolfenden R. Contribution of enzyme-phosphoribosyl contacts to catalysis by orotidine 5'-phosphate decarboxylase. Biochemistry 2000;39:8113–8118. [PubMed: 10889016]
11. Lolis E, Petsko GA. Crystallographic analysis of the complex between triosephosphate isomerase and 2-phosphoglycolate at 2.5-Å. resolution: implications for catalysis. Biochemistry 1990;29:6619–6625. [PubMed: 2204418]
12. Davenport RC, Bash PA, Seaton BA, Karplus M, Petsko GA, Ringe D. Structure of the triosephosphate isomerase-phosphoglycolohydroxamate complex: an analog of the intermediate on the reaction pathway. Biochemistry 1991;30:5821–5826. [PubMed: 2043623]
13. Cannon WR, Benkovic SJ. Solvation, reorganization energy, and biological catalysis. J. Biol. Chem 1998;273:26257–26260. [PubMed: 9756847]
14. Warshel A. Electrostatic Origin of the Catalytic Power of Enzymes and the Role of Preorganized Active Sites. J. Biol. Chem 1998;273:27035–27038. [PubMed: 9765214]
15. Plaut B, Knowles JR. pH-Dependence of the triose phosphate isomerase reaction. Biochem. J 1972;129:311–320. [PubMed: 4643319]
16. Bentley P, Dickinson FM, Jones IG. Purification and properties of rabbit muscle L-glycerol 3-phosphate dehydrogenase. Biochem. J 1973;135:853–859. [PubMed: 4778280]
17. Reynolds SJ, Yates DW, Pogson CI. Dihydroxyacetone phosphate. Its structure and reactivity with α-glycerolphosphate dehdyrogenase, aldolase and triose phosphate isomerase and some possible metabolic implications. Biochem. J 1971;122:285–297. [PubMed: 4330197]
18. Bentley P, Dickinson FM. A study of the kinetics and mechanism of rabbit muscle L-glycerol 3-phosphate dehydrogenase. Biochem. J 1974;143:19–27. [PubMed: 4377219]
19. Black WJ. Kinetic studies on the mechanism of cytoplasmic L-α-glycerophosphate dehydrogenase of rabbit skeletal muscle. Can. J. Biochem. Phys 1966;44:1301–1317.
20. Suresh S, Turley S, Opperdoes FR, Michels PAM, Hol WGH. A potential target enzyme for trypanocidal drugs revealed by the crystal structure of NAD-dependent glycerol-3-phosphate dehydrogenase from. Leishmania mexicana., Structure 2000;8:541–552.
21. Ou X, Ji C, Han X, Zhao X, Li X, Mao Y, Wong L-L, Bartlam M, Rao Z. Crystal structures of human glycerol 3-phosphate dehydrogenase 1 (GPD1). J. Mol. Biol 2006;357:858–869. [PubMed: 16460752]
22. Zhang Z, Sugio S, Komives EA, Liu KD, Knowles JR, Petsko GA, Ringe D. Crystal structure of recombinant chicken triosephosphate isomerase-phosphoglycolohydroxamate complex at 1.8-Å resolution. Biochemistry 1994;33:2830–2837. [PubMed: 8130195]
23. Begley TP, Appleby TC, Ealick SE. The structural basis for the remarkable catalytic proficiency of orotidine 5'-monophosphate decarboxylase. Curr. Opin. Struct. Biol 2000;10:711–718. [PubMed: 11114509]
24. Richard JP, Amyes TL. On the importance of being zwitterionic: enzymic catalysis of decarboxylation and deprotonation of cationic carbon. Bioorg. Chem 2004;32:354–366. [PubMed: 15381401]
25. Hine, J. Structural effects on equilibria in organic chemistry. New York: John Wiley & Sons; 1975.

26. Kohen A, Klinman JP. Enzyme catalysis: beyond classical paradigms. Acc. Chem. Res 1998;31:397–404.

27. Ray WJ Jr, Long JW. Thermodynamics and mechanism of the PO_3 transfer process in the phosphoglucomutase reaction. Biochemistry 1976;15:3993–4006. [PubMed: 963018]

28. Jencks WP. On the attribution and additivity of binding energies. Proc. Natl. Acad. Sci. U. S. A 1981;78:4046–4050. [PubMed: 16593049]

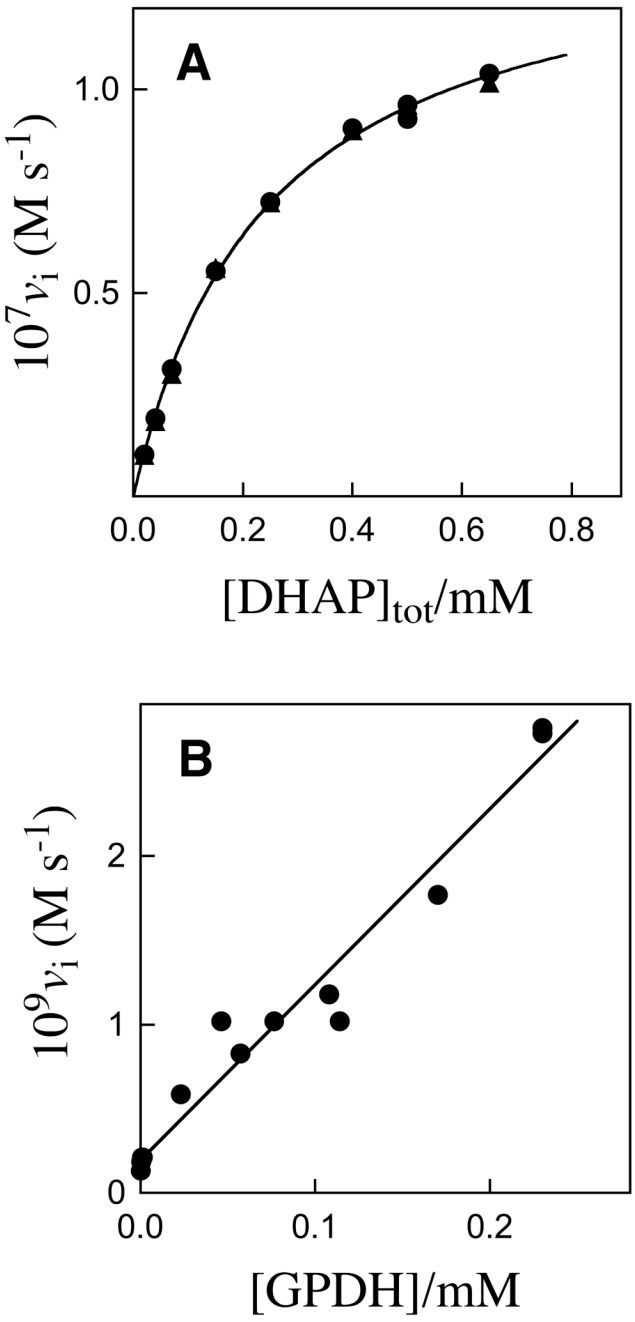

Figure 1.

A. Dependence of the initial velocity, v_i, of the reduction of DHAP by NADH catalyzed by GPDH (1.1 nM) on the total concentration of DHAP in the presence of 0.10 mM (▲) or 0.20 mM (●) NADH at pH 7.5, 25 °C and I = 0.12 (NaCl). **B**. Dependence of the initial velocity, v_i, of the reduction of GLY (20 mM total, 1.2 mM free carbonyl form) by NADH (0.20 mM) on the concentration of GPDH at pH 7.5, 25 °C and I = 0.12 (NaCl).

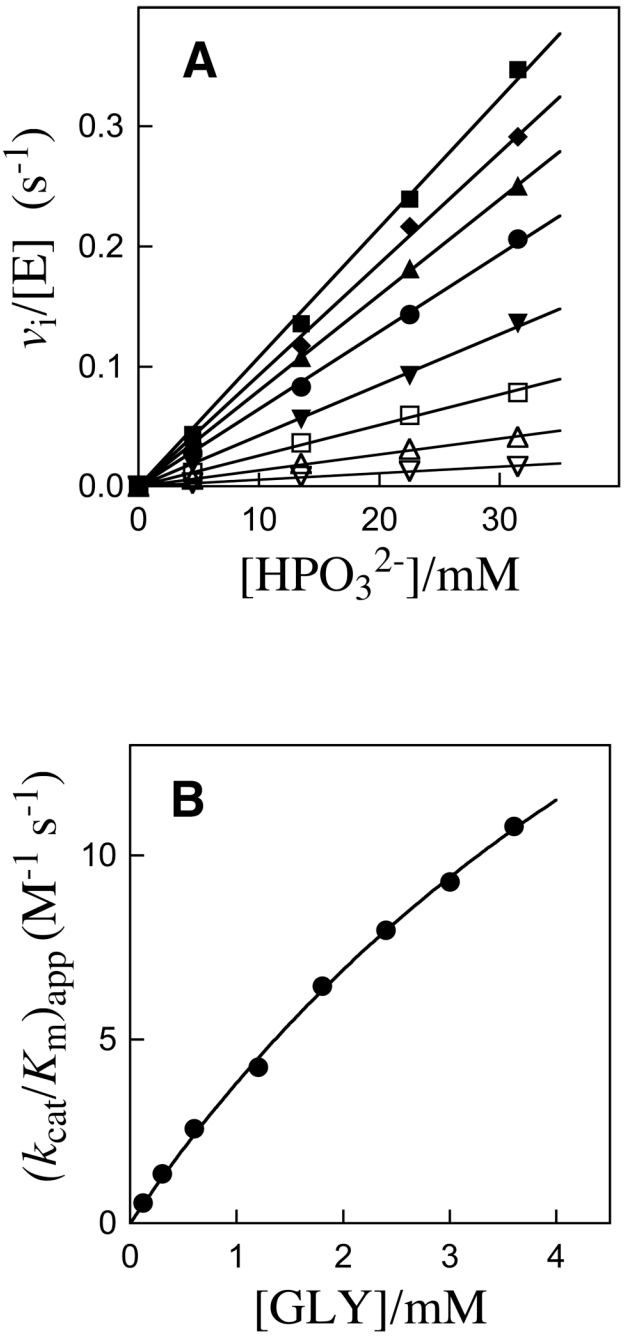

Figure 2.

A. Dependence of v_i/[E] for the reduction of GLY by NADH (0.20 mM) catalyzed by GPDH (0.6 μM) on the concentration of exogenous phosphite dianion at pH 7.5, 25 °C and I = 0.12 (NaCl). Concentrations of GLY (free carbonyl from) were: ▽ [GLY] = 0.12 mM; △ [GLY] = 0.30 mM; □ [GLY] = 0.60 mM; ▼ [GLY] = 1.2 mM; ● [GLY] = 1.8 mM; ▲ [GLY] = 2.4 mM; ◆ [GLY] = 3.0 mM; ■ [GLY] = 3.6 mM. **B**. Dependence of the apparent second-order rate constant $(k_{cat}/K_m)_{app}$ for the phosphite-activated GPDH-catalyzed reduction of GLY by NADH (0.20 mM) on the concentration of GLY at pH 7.5, 25 °C and I = 0.12 (NaCl), calculated as the slopes of the correlations in Figure 2A.

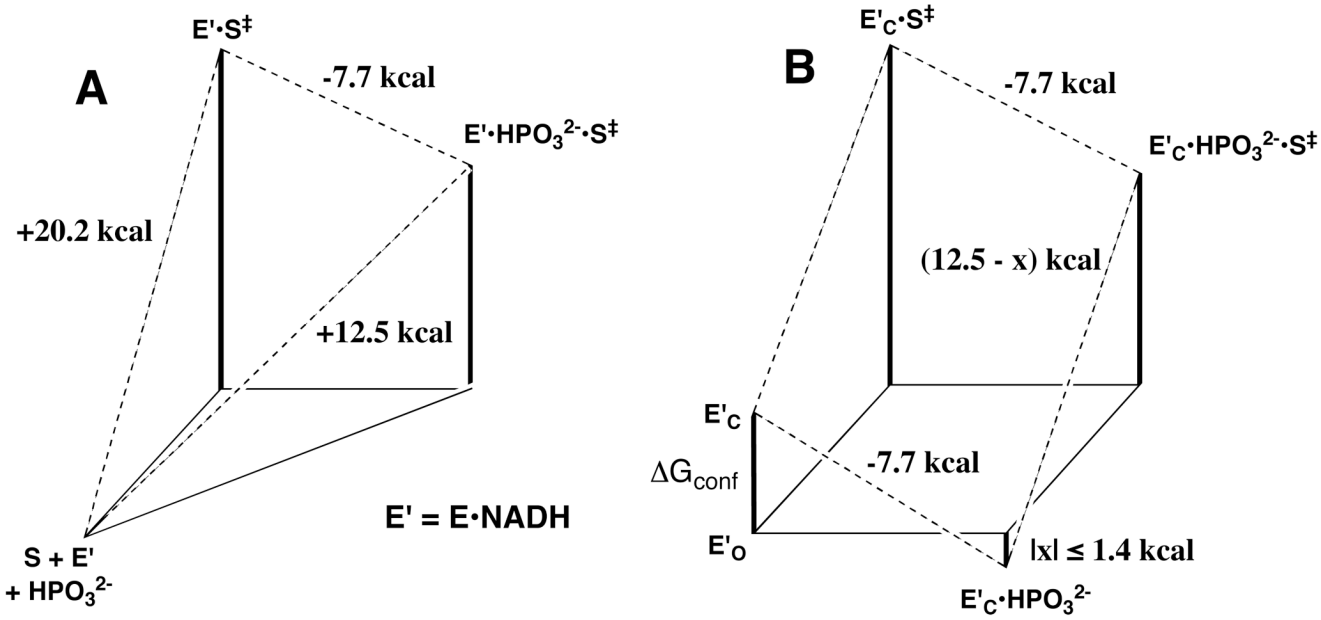

Figure 3.

A. Free energy diagram for turnover of the truncated neutral substrate GLY (S) by the binary GPDH•NADH complex (E') and for the same reaction activated by the binding of exogenous phosphite dianion (HPO_3^{2-}). Activation free energies were calculated using the Eyring equation at 298 K. The weakly bound Michaelis complex E'•HPO_3^{2-} is not shown, because the stability of this complex is not defined by our experiments. **B**. Free energy diagram illustrating our proposed model for activation of E' towards reduction of GLY by the binding of HPO_3^{2-}. Binding energies are defined to be negative when the binding is thermodynamically favorable. The *difference* between the total intrinsic phosphite binding energy of −7.7 kcal/mol and the observed binding energy× > −1.4 kcal/mol for binding of HPO_3^{2-} to the *inactive open* enzyme E'_O to give the *active closed* enzyme E'_C•HPO_3^{2-} is the binding energy that is used to convert E'_O to E'_C. The observed value of $\Delta G^{\ddagger}$ = +20.2 kcal/mol for turnover of GLY (Figure 3A) has been partitioned into $\Delta G^{\ddagger}$ for reduction of GLY by E'_C and ΔG_{conf} for the unfavorable conformational change that converts E'_O to E'_C.

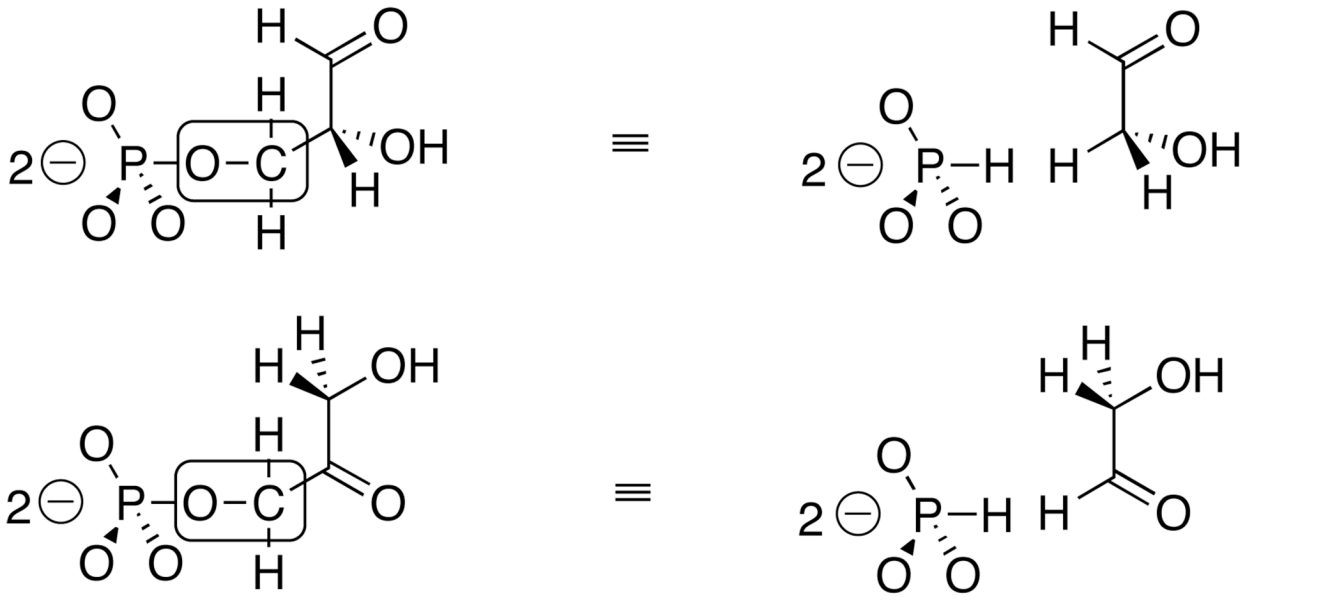

Scheme 1.

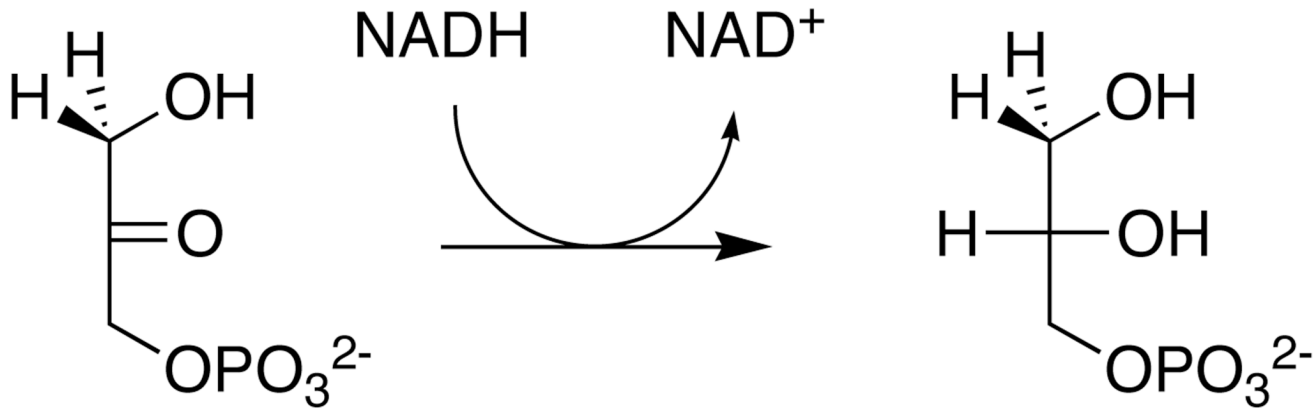

Scheme 2.

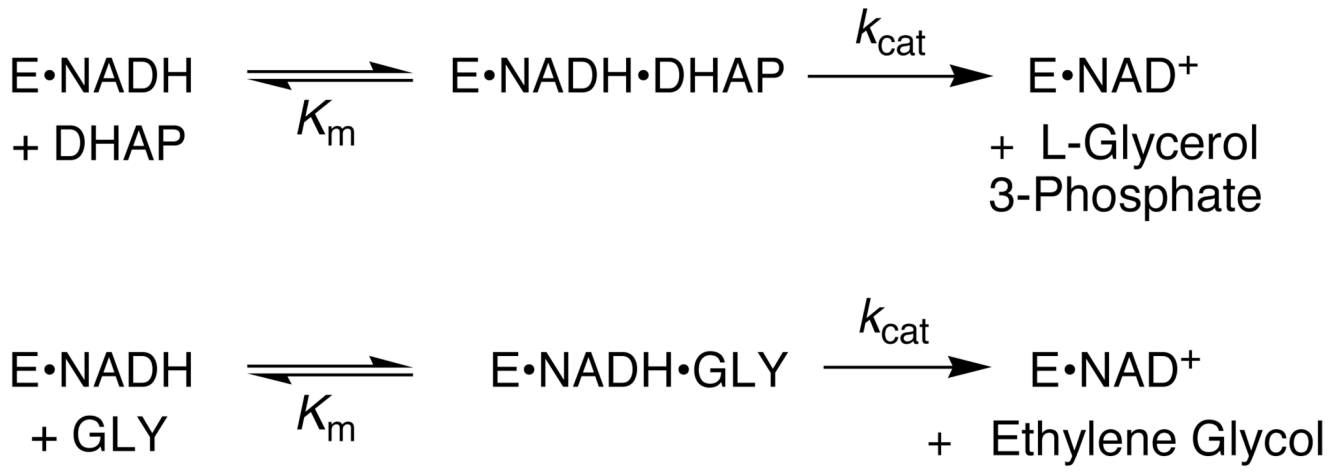

Scheme 3.

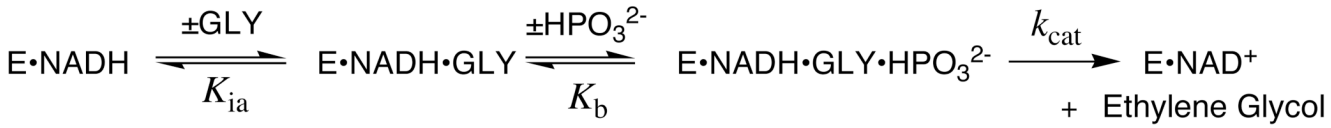

Scheme 4.

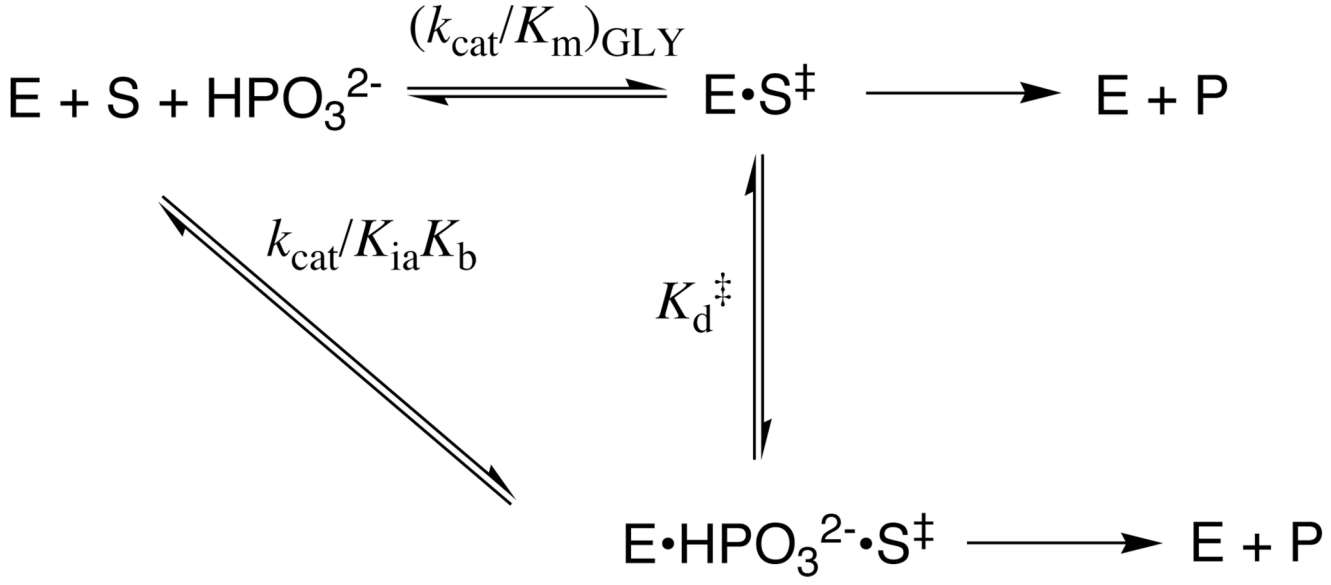

Scheme 5.

Table 1

Kinetic Parameters for Reduction of Dihydroxyacetone Phosphate and Glycolaldehyde Catalyzed by GPDH and for Activation by Phosphite Dianion[a]

Substrate	Activator	K_m[b] mM	k_{cat} s^{-1}	k_{cat}/K_m M^{-1} s^{-1}	K_d[c] M	$k_{cat}/K_{ia}K_b$ M^{-2} s^{-1}
DHAP[d]		0.13	130	1.0×10^6		
GLY[e]				$(8.7 \pm 0.5) \times 10^{-3}$		
GLY[f]	HPO_3^{2-}	8 ± 1			> 0.1	4300 ± 700

[a] At pH 7.5 (10 mM TEA buffer), 25 °C and I = 0.12 (NaCl).

[b] Values of K_m refer to the free carbonyl form of DHAP or GLY.

[c] Dissociation constant for the phosphite dianion activator.

[d] Kinetic parameters determined from data shown in Figure 1A.

[e] Kinetic parameters determined from data shown in Figure 1B.

[f] Kinetic parameters determined from data shown in Figure 2.

Table 2

A Comparison of the Intrinsic Phosphate Binding Energy and the Observed and Total Intrinsic Phosphite Binding Energy for Enzyme-Catalyzed Decarboxylation, Proton Transfer and Hydride Transfer Reactions[a]

Enzymatic Reaction	$(k_{cat}/K_m)_{SPi}$[b] M^{-1} s^{-1}	$(k_{cat}/K_m)_S$[c] M^{-1} s^{-1}	Intrinsic Phosphate Binding Energy[d]	$(k_{cat}/K_m)_S/K_d$[e] M^{-2} s^{-1}	Observed and Total Intrinsic Phosphite Binding Energy[f]
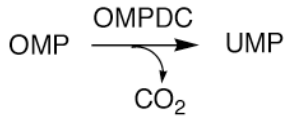 Decarboxylation[g]	9.4×10^6	0.021	−11.8 kcal/mol	12,000	−1.2 kcal/mol −7.8 kcal/mol
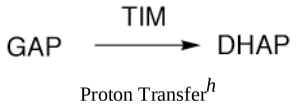 Proton Transfer[h]	2.4×10^8	0.26	−12.2 kcal/mol	4900	−1.9 kcal/mol −5.8 kcal/mol
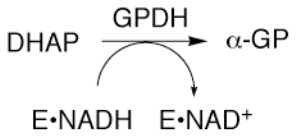 Hydride Transfer[i]	1.0×10^6	0.0087	≤ −11.0 kcal/mol	4300	> −1.4 kcal/mol −7.7 kcal/mol

[a] Binding energies are defined to be negative when the binding is thermodynamically favorable.

[b] Second-order rate constant for turnover of the whole phosphorylated natural substrate by the free enzyme.

[c] Second-order rate constant for turnover of the neutral truncated substrate lacking a phosphodianion group by the free enzyme.

[d] Calculated from the rate constant ratio $(k_{cat}/K_m)_{SPi}/(k_{cat}/K_m)_S$.

[e] Third-order rate constant for enzyme-catalyzed reaction of the neutral truncated substrate activated by phosphite dianion.

[f] Energy for binding of phosphite dianion to the free enzyme (upper number) and to the transition state complex $E•S^{‡}$ (lower number).

[g] Data from Ref. 6.

[h] Data from Ref. 8.

[i] Data from this work.